Adiabatic Elimination in Strong Field Light Matter Coupling

Brian Kaufman,[1] Tamás Rozgonyi,[2,3] Philipp Marquetand,[4,5,6] and Thomas Weinacht[1]
[1] *Department of Physics and Astronomy, Stony Brook University, Stony Brook NY 11794-3800, USA*
[2] *Wigner Research Centre for Physics, P.O. Box 49, H-1525 Budapest, Hungary*
[3] *Research Centre for Natural Sciences, Magyar tudósok krt. 2, H-1117 Budapest, Hungary*
[4] *University of Vienna, Faculty of Chemistry, Institute of Theoretical Chemistry, Währinger Str. 17, 1090 Wien, Austria*
[5] *Vienna Research Platform on Accelerating Photoreaction Discovery, University of Vienna, Währinger Str. 17, 1090 Wien, Austria and*
[6] *University of Vienna, Faculty of Chemistry, Data Science @ Uni Vienna, Währinger Str. 29, 1090 Wien, Austria*
(Dated: December 1, 2020)

We explore the validity of adiabatic elimination in the derivation of an essential-states representation of the time-dependent Schrödinger equation in the presence of a strong laser field. We consider the elimination of off resonant states in generating an effective two level description of the light matter interaction, where the initial and final states are two-photon resonant. The treatment is non-perturbative and can be generalized to N-photon absorption.

I. INTRODUCTION

In time-resolved spectroscopy and non-linear optics, the coupling between a strong-field laser pulse and the molecule of interest takes center stage [1–3]. An important tool in dealing with strong laser-molecule coupling is adiabatic elimination (AE), which allows one to derive multi-photon Rabi frequencies and dynamic Stark shifts, as well as describe the laser-molecule interaction in terms of a small group of "essential states" [4–17]. AE can also be applied in the calculation of "multiphoton" decay channels, such as the two-photon decay of the Hydrogen 2s state [18], or for coupling control in waveguides [19] and is the starting point for developing more accurate approximations for quantum computing simulations [20–22].

If one considers the full time-dependent Schrödinger equation (TDSE) in the basis of field-free molecular states, then the idea is to eliminate those "intermediate" molecular states which do not play an important role in the dynamics - i.e. those which are not significantly populated during the interaction with the laser field. These states are so far off resonance that any population that is transferred to the state is rapidly transferred back to the initial state as the interaction switches between stimulated absorption and emission at the detuning frequency, $\Delta = \omega_0 - (E_i - E_0)$, where E_i and E_0 represent the energies of the ground and intermediate states.

Our goal is to examine the validity of removing such "far off resonant" states in detail by comparing numerical integration of the TDSE with all states considered explicitly (exact treatment) vs calculations where the off-resonant states have been adiabatically eliminated. We show how cancellation of errors enables accurate calculations with AE even when the validity of the approximation is in question. This supports the use of AE even for very short (i.e. few cycle) pulses which do not fulfill the slowly varying envelope approximation.

II. MODEL SYSTEM

In the following, we focus on a simple model system. We divide the eigenstates of the field-free molecule into two groups. An initial ground state, $|\psi_g\rangle$, and an excited state, $|\psi_e\rangle$, which are "n-photon resonant" ($E_e - E_g = n\omega$ in atomic units), and all of the other "intermediate" states, $|\psi_i\rangle$, of the system which are off resonant but dipole coupled to both the initial and final states. For our simulations, we restrict ourselves to a model with two-photon transitions and one intermediate state. These are illustrated in the bottom left corner of Fig. 1. Further details can be found in the appendix. We ignore vibrations here, but they have been included in a separate paper [23].

III. ADIABATIC ELIMINATION

The traditional formulation for adiabatic elimination is to assume a slowly varying field envelope and large detuning of the intermediate state, such that the variation in the Rabi frequency, $\dot{\chi}$, between i and g or e and i has to be much smaller than the Rabi frequency, χ, times the detuning between g and i, or e and i, Δ_{ig} or Δ_{ei} (i.e. $\dot{\chi}/\chi \ll \Delta$) [1, 14]. Here we revisit this approximation, and calculate the errors that one accumulates with AE when the approximation is not strictly valid. We present a brief derivation of the TDSE with AE, illustrating exactly what approximations are made to create the adiabatically eliminated system. We start by writing the time-dependent wavefunctions in terms of the field-free electronic eigenstates:

$$|\Psi(t)\rangle = \sum_{n=g,e,i} c_n(t) e^{-i\omega_n t} |\psi_n\rangle \tag{1}$$

where $c_n(t)$ is the complex amplitude of the n^{th} electronic eigenstate, with n representing the ground state g, the excited state e, or any intermediate states i. The TDSE

is then:

$$i\dot{c_m} = \sum_{n=g,e,i} c_n(t)e^{-i\omega_{mn}t} \langle\psi_m| H_{int} |\psi_n\rangle \tag{2}$$

where $\omega_{mn} \equiv \omega_m - \omega_n$ and H_{int} is the Hamiltonian of the system including the molecule-field interaction.

Up to this point the TDSE is general, but not particularly useful because of the large number of intermediate states that are involved, leading to a potentially very large Hamiltonian matrix. The idea in AE is to eliminate all of the states i from the TDSE, while taking into account the role that they play in generating multi-photon couplings and dynamic Stark shifts. We focus here on an initial and final state which are two-photon coupled. The extension to higher order couplings is straightforward but tedious. As mentioned above, we focus here on an initial and final state which are two-photon coupled via a single intermediate state, i, understanding that this can represent many states and that in general one needs to sum over a large number of such states in the derivation in order to accurately calculate the multi-photon couplings and Stark shifts.

Using Eq. 2 the TDSE for this system can be written as:

$$i\dot{c_g} = c_i(t)e^{+i\omega_{gi}t} \langle\Psi_g| H_{int} |\Psi_i\rangle \tag{3a}$$

$$\begin{aligned} i\dot{c_i} = {} & c_g(t)e^{-i\omega_{gi}t} \langle\Psi_i| H_{int} |\Psi_g\rangle \\ & + c_e(t)e^{-i\omega_{ei}t} \langle\Psi_i| H_{int} |\Psi_e\rangle \end{aligned} \tag{3b}$$

$$i\dot{c_e} = c_i(t)e^{+i\omega_{ei}t} \langle\Psi_e| H_{int} |\Psi_i\rangle \tag{3c}$$

where the coupling is given by:

$$\langle\Psi_n| H_{int} |\Psi_m\rangle = -\frac{1}{2}\chi_{nm}(t)(e^{+i\omega_0 t} + e^{-i\omega_0 t}) \tag{4}$$

with $\chi_{nm}(t) = \mu_{nm}E(t)$, where μ_{nm} is an element of the transition dipole moment matrix and $E(t)$ is the time dependent electric field amplitude. We drop the explicit time dependence of χ_{nm} for ease of notation.

When written out explicitly by plugging the coupling (Eq. 4) into Eqs. 3 the complex exponentials for the molecule $e^{\pm i\omega_{gi}t}$, $e^{\pm i\omega_{ei}t}$ and light $e^{\pm i\omega_0 t}$ combine such that we can define the AE frequencies: $\omega_{g,e\pm} \equiv \omega_{g,ei} \pm \omega_0$, and using these rewrite Eqs. 3 as:

$$i\dot{c_g} = c_i(t)(-\frac{\chi_{gi}}{2})(e^{+i\omega_{g+}t} + e^{+i\omega_{g-}t}) \tag{5a}$$

$$\begin{aligned} i\dot{c_i} = {} & c_g(t)(-\frac{\chi_{gi}}{2})(e^{-i\omega_{g+}t} + e^{-i\omega_{g-}t}) \\ & + c_e(t)(-\frac{\chi_{ei}}{2})(e^{-i\omega_{e+}t} + e^{-i\omega_{e-}t}) \end{aligned} \tag{5b}$$

$$i\dot{c_e} = c_i(t)(-\frac{\chi_{ei}}{2})(e^{+i\omega_{e+}t} + e^{+i\omega_{e-}t}) \tag{5c}$$

The process of adiabatic elimination begins by directly integrating the rapidly oscillating, off-resonant intermediate state (Eq. 5b):

$$\begin{aligned} c_i(t) &= -\frac{1}{2i}\int_{-\infty}^{t} dt' \big[\;\; c_g(t')\chi_{gi}e^{-i\omega_{g+}t'} + c_g(t')\chi_{gi}e^{-i\omega_{g-}t'} \\ &\qquad + c_e(t')\chi_{ei}e^{-i\omega_{e+}t'} + c_e(t')\chi_{ei}e^{-i\omega_{e-}t'} \big] \\ &= -\frac{1}{2i}\int_{-\infty}^{t} dt' \big[\;\; g_+ + g_- + e_+ + e_- \big] \end{aligned} \tag{6}$$

This leads to four separate integrals where we define the integrands as g_+, g_-, e_+, and e_- based on the AE frequencies. We can evaluate these four integrals by the usual integration by parts: $\int UdV = UV - \int VdU$. If we take $\int dt' g_-$ as an example then $U = \chi_{ig}c_g(t')$ and $dV = e^{-i\omega_{g-}t}$, resulting in the integral:

$$\begin{aligned} \int_{-\infty}^{t} dt' g_- = {} & \chi_{ig}c_g(t')\frac{e^{-i\omega_{g-}t'}}{-i\omega_{g-}} \\ & - \int_{-\infty}^{t} dt' \frac{d}{dt}[\chi_{ig}c_g(t')]\frac{e^{-i\omega_{g-}t'}}{-i\omega_{g-}} \end{aligned} \tag{7}$$

The usual approach to adiabatic elimination can be expressed in terms of $\dot{\chi}_{ie,g}/\chi_{ie,g} \ll \omega_{g,e\pm}$ such that we can neglect the $\int VdU$ term, since it is an integral of a product of slowly and rapidly varying terms. However, a more precise condition for adiabatic elimination can be derived from Eq. 7 by performing integration by parts a second time. The U term now contains a derivatve, $U = \frac{d}{dt}\chi_{ig}c_g(t')$, while the dV term remains the same, $dV = e^{-i\omega_{g-}t}$, yielding:

$$\int_{-\infty}^{t} dt' g_- = \chi_{ig}c_g(t')\frac{e^{-i\omega_{g-}t'}}{-i\omega_{g-}} \tag{8a}$$

$$+ \frac{d}{dt}[\chi_{ig}c_g(t')]\frac{e^{-i\omega_{g-}t'}}{\omega_{g-}^2} \tag{8b}$$

$$- \int_{-\infty}^{t} dt' \frac{d^2}{dt^2}[\chi_{ig}c_g(t')]\frac{e^{-i\omega_{g-}t'}}{\omega_{g-}^2} \tag{8c}$$

This approach now allows us to directly compare the different terms in Eq. 7: 8a and 8b. The approximation requires that 8b be much smaller than 8a, and assuming that the second derivative of the envelope will vary even slower than the first, 8c can be neglected. Thus, the approximation can be written as:

$$\left| \frac{1}{\chi_{ig}c_g(t)} \left(\frac{dc_g}{dt}\chi_{ig}(t) + \frac{d\chi_{ig}}{dt}c_g(t) \right) \right| \ll |\omega_{g-}| \tag{9}$$

where an appropriate swap of g/e and $+/-$ yield a similar inequality for the other three AE frequencies.

Although similar to the traditional approximation, this revised statement of the approximation contains an additional term, which leads to cancellation of errors if the two terms have different signs. We note that the sign of the terms can also vary as a function of time since the

derivative of the Rabi frequency changes at the peak of the pulse and the state coefficients are not always real and positive.

If Eq. 9 is satisfied then the $\int V dU$ term can be removed from each of the four integrals leaving us with the intermediate state written as:

$$\begin{aligned} c_i(t) =& \frac{-\chi_{gi}}{2} c_g(t) \left[\frac{e^{-i\omega_{g+}t}}{\omega_{g+}} + \frac{e^{-i\omega_{g-}t}}{\omega_{g-}} \right] \\ &+ \frac{-\chi_{ei}}{2} c_e(t) \left[\frac{e^{-i\omega_{e+}t}}{\omega_{e+}} + \frac{e^{-i\omega_{e-}t}}{\omega_{e-}} \right] \end{aligned} \tag{10}$$

Now we plug this equation (Eq. 10) back into the differential equations for $c_g(t)$ and $c_e(t)$, Eq. 5a and 5c, respectively. The next step is to make the two-photon rotating wave approximation to eliminate the rapidly oscillating terms which is to say that any oscillation faster than the two-photon detuning, $\Delta_2 = \omega_{eg} - \omega_0$, is removed. See the appendix for the complete derivation continuing from Eq. 10. The system resulting from AE + the two-photon rotating wave approximation (AER) can thus be written as a system of two coupled first order differential equations:

$$i\dot{c_g} = c_g(t) \frac{\chi_{gi}^2}{2} \frac{\omega_{gi}}{\omega_{gi}^2 - \omega_0^2} + c_e(t) \frac{1}{4} \frac{\chi_{gi}\chi_{ei}}{\omega_{ei} - \omega_0} e^{-i\Delta_2 t} \tag{11a}$$

$$i\dot{c_e} = c_e(t) \frac{\chi_{ei}^2}{2} \frac{\omega_{ei}}{\omega_{ei}^2 - \omega_0^2} + c_g(t) \frac{1}{4} \frac{\chi_{ei}\chi_{gi}}{\omega_{gi} + \omega_0} e^{+i\Delta_2 t} \tag{11b}$$

or more concisely in terms of the dynamic Stark shift $\omega_{g,e}^S(t)$ and the two-photon Rabi frequency $\Omega(t)$:

$$\begin{aligned} i\dot{c_g} &= c_g(t)\omega_g^S(t) + c_e(t)\tilde{\Omega}(t)e^{-i\Delta_2 t} \\ i\dot{c_e} &= c_e(t)\omega_e^S(t) + c_g(t)\Omega(t)e^{+i\Delta_2 t} \end{aligned} \tag{12}$$

In order to quantify the error associated with AE, we numerically integrate the full system of equations given by Eq. 5 (exact solution), as well as the equations after AER given by Eq. 11. The results of these calculations are shown in Fig. 1. The top panel shows the laser pulse intensity as a function of time, where the pulse has a Gaussian profile with a peak intensity of 2/3 TW/cm^2 and pulse duration of 30 fs. The bottom panel shows the state populations as a function of time, where the population is given by $P_n(t) = |c_n(t)|^2$. In this panel there is an inset showing the energy level diagram where the one-photon detuning ($\Delta = E_i - E_g - \nu_0$) is 200 THz. These parameters were chosen such that there was a large population transfer to the excited state and that the simulation would meet the standard adiabatic criteria as the 30 fs pulse sustains a bandwidth of $\approx$ 15 THz which is much less than the detuning. Full model parameters are given by Table II in the appendix.

The solid curves of Fig. 1 show the solution to integrating the full system Eq. 5. As expected, the intermediate state population shows rapid oscillations with no population remaining in the state at the end of the pulse. This outcome reflects the fact that the intermediate state acts

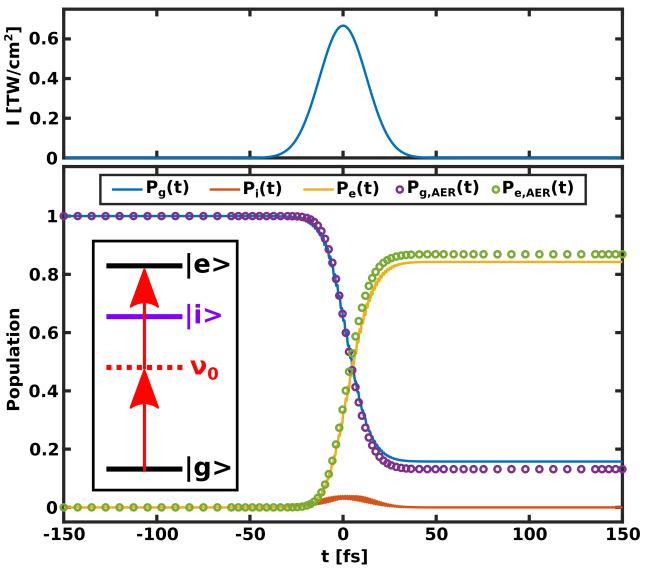

FIG. 1. Populations as a function of time for a three level system with laser induced coupling. Top panel: laser intensity vs. time. Bottom panel: populations vs. time. Solid curves correspond to the full system and dotted curves correspond to the AER system. The inset shows the energy level diagram for the three level system.

as a mediator between the ground and excited states, but has no lasting effect. This circumstance forms the basis for AE, where we eliminate the intermediate state and move its mediating effects to the dynamic Stark shift and two-photon Rabi frequencies.

The dotted curves show the solution to the AER system Eq. 11 where the intermediate state has been adiabatically eliminated. The agreement between the full system and the AER system is quite good with a population error, $(P_e^{Full} - P_e^{AER})/P_e^{Full}$, of only 2.5%.

IV. VALIDITY OF THE APPROXIMATION

We have found that AE works (producing relatively small errors in comparison to integration of the full TDSE) even when the slowly varying envelope approximation (SVEA) is not strictly valid, as illustrated in figure 1. Here, we examine the validity of the approximation in more detail by testing its limits. In Fig. 2 we calculate the populations of the states for four different pulse durations. The intensity was adjusted to keep the pulse area constant for the four simulations. In the top left panel, we show the results for a 300 fs pulse, for which the SVEA is valid, given an intermediate state detuning of 200 THz and a pulse envelope bandwidth of less than 2 THz. The solutions to the full TDSE and the AER equations overlap perfectly. As the pulse duration is decreased, the approximation becomes worse and we see some accumulation of error in compar-

ing the solutions to the TDSE and the AER equations. However, the disagreement between the TDSE and AER solutions remains rather small, even for a 10 fs pulse, where the SVEA is clearly violated. Furthermore, the solutions are still relatively close even for the dramatic case of a roughly single cycle pulse, which grossly violates the SVEA.

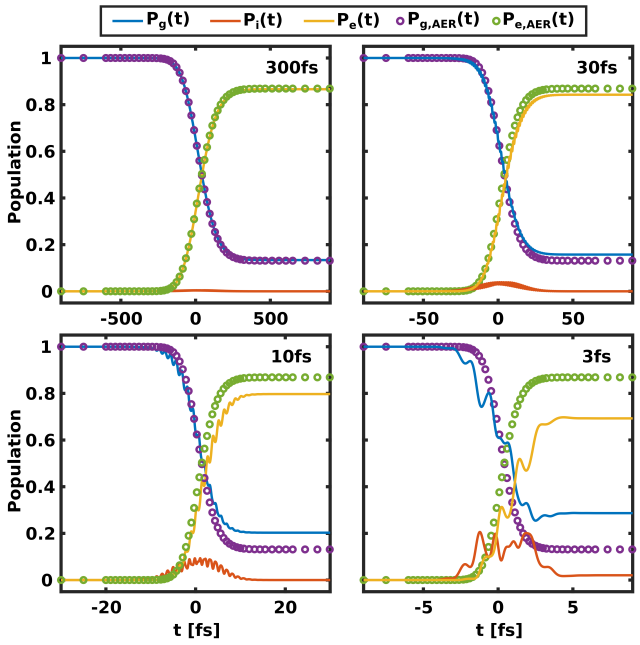

FIG. 2. Adiabatic Elimination using different pulse durations while maintaining a constant pulse area. Pulse durations shown: 300fs (top left), 30fs (top right), 10fs (bottom left), 3fs (bottom right).

So far we have only discussed how the approximation works in the case of varying pulse duration. A similar analysis can be done by varying the intermediate state detuning, which we show in Appendix Fig. 5. Looking at Eq. 9, one can show that the approximation can be discussed in terms of either the pulse duration (dictated by the pulse bandwidth for a transform limited pulse) based on $d\chi/dt$ from the LHS of the inequality or the one-photon detuning based on $\omega_{g,e\pm}$ from the RHS and that these are equivalent pictures.

A more thorough analysis of the population error, given in appendix Fig. 6, shows that there is a smooth decrease in error with increasing pulse duration. This highlights the fact that there is nothing special about the particular pulse durations discussed here. Adiabatic elimination works even when the envelope does not vary very slowly compared to the central frequency.

V. INTERPRETATION

In order to understand why AE works so well we need to take a closer look at the approximation. The SVEA is essentially equivalent to assuming that each term in the LHS of Eq. 9 is smaller than the RHS. However, the errors associated with the sum of the two terms can be small even when the SVEA is not valid due to cancellation between the two terms. We return to the integration by parts from Eq. 7 in particular focusing on the $\int VdU$ term because this term describes the error in AE. Expanding this term based on the product rule yields:

$$\int (VdU)^{g-} = \int_{-\infty}^{t} dt' \frac{d}{dt}[\chi_{ig} c_g(t')] \frac{e^{-i\omega_{g-}t'}}{-i\omega_{g-}} \tag{13a}$$

$$= \int_{-\infty}^{t} dt' \frac{e^{-i\omega_{g-}t'}}{-i\omega_{g-}} \frac{d\chi_{ig}}{dt} c_g(t') + \int_{-\infty}^{t} dt' \frac{e^{-i\omega_{g-}t'}}{-i\omega_{g-}} \frac{dc_g(t')}{dt} \chi_{ig} \tag{13b}$$

$$= \int (VdU)_1^{g-} + \int (VdU)_2^{g-} \tag{13c}$$

where this equation is representative of the other three terms $g+$, $e-$, and $e+$. This expansion highlights the importance of the product rule and gives us the first level of cancellation of errors throughout the approximation.

In order to emphasize this cancellation of errors, we calculate each contribution to the intermediate state coefficient (all four UV terms and all eight $\int VdU$ terms) and use these to determine each contribution to the excited state coefficient ($c_e(t)$) by plugging each into the integral solving for the excited state:

$$c_e(t) = -\frac{1}{2i} \int_{-\infty}^{t} dt' c_i(t') \chi_{ei} (e^{+i\omega_{e+}t'} + e^{+i\omega_{e-}t'}) \tag{14}$$

For example, we insert $c_i(t') = \int (VdU)_1^{g-}$ into Eq. 14 to determine this term's contribution to the $c_e(t)$. This term is plotted in the upper left panel of Fig. 3 in black for the system described in Fig. 1. We then calculate the contribution to $c_e(t)$ from the remaining seven $\int VdU$ terms which are plotted as a function of time in Fig. 3. For clarity, each contribution to $c_e(t)$ is normalized to the total $c_e(t)$ used to calculate the population.

Fig. 3 is divided into four panels marked $g-$ (top left), $e+$ (top right), $g+$ (bottom left), and $e-$ (bottom right). These correspond to the $\int VdU$ term for the four integrals given by Eq. 6. The black and grey curves represent this integral separated via the product rule as shown in the example Eq. 13, where the colored curves represent the sum of these two terms.

The top two panels ($g-$ and $e+$) show little contribution due to $\int (VdU)_1$, (i.e. the derivative of the field) and are thus dominated by the second term (the derivative of the coefficient) but this term is quite small, being less than 1%. We can attribute this to the fast oscillation frequencies $\omega_{g-} = -1000$ THz and $\omega_{e}+ = +600$ THz which lead to very little population transfer.

The bottom two panels ($g+$ and $e-$) tell a much more interesting story. Both show a 2% error due to the dc/dt term, but this is then cancelled by the $d\chi/dt$ term, yielding a reduced total error of $\approx 1\%$.

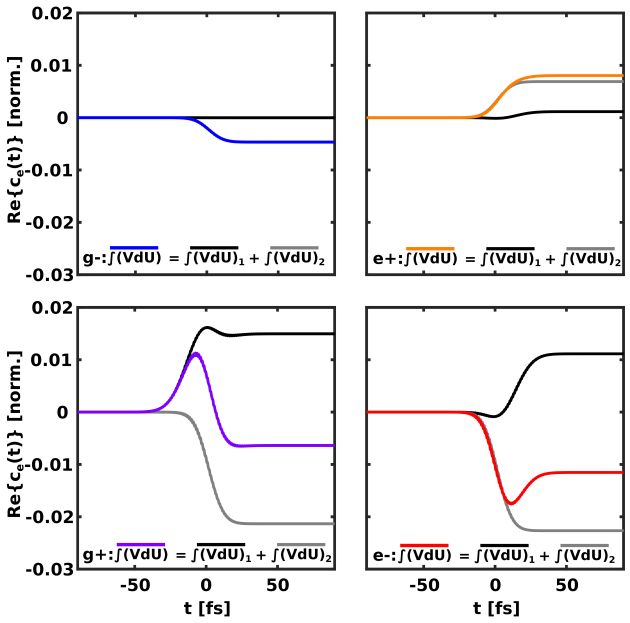

FIG. 3. Excited state coefficient contributions from the $\int VdU$ terms split by the product rule (RHS Eq. 13) and normalized to the total final excited state coefficient. The imaginary complement is given by appendix Fig. 7.

The discussion above highlights a first level of error cancellation. As shown in Eq. 6 the four colored curves in Fig. 3 must also be summed. Fig. 4 reproduces these four curves and additionally shows their sum as the black dashed line. Here, it is quite striking to see that the $e+$ term has the opposite sign compared to the other three, which introduces a further cancellation of errors. This sign difference arises due to the denominator in the $\int VdU$. The denominator is the AE frequency which is ω_g- in Eq. 13. The four AE frequencies are then $\omega_{g-} = -1000$ THz, $\omega_{g+} = \omega_{e-} = -200$ THz, and $\omega_{e+} = +600$ THz. The $e+$ carries the opposite sign to the others, providing additional cancellation of errors in AE. Furthermore, we see that there is cancellation in time due to the change in sign of the derivative of the Rabi frequency, as discussed below Eq. 9. This cancellation in time is even more pronounced in the imaginary part of the coefficients, as shown in figures 7 and 8 in the appendix. These multiple levels of cancellation reduce the total error due to adiabatic elimination, and allow calculations that make use of AE to yield accurate results even when the traditional statement of the approximation is not strictly valid.

VI. CONCLUSION

Adiabatic elimination often works much better than expected based on the traditional formulation of the approximation in terms of the SVEA. In order to understand why, we have examined the approximation in greater detail, uncovering multiple cancellations of errors. This provides a deeper understanding of the approximation, and validates the application of AE even when the SVEA fails.

ACKNOWLEDGMENTS

This work has been supported by National Science Foundation under award number 1806294. It was also partly supported by the Government of Hungary and the European Regional Development Fund under Grant No. VEKOP-2.3.2-16-2017-00015.

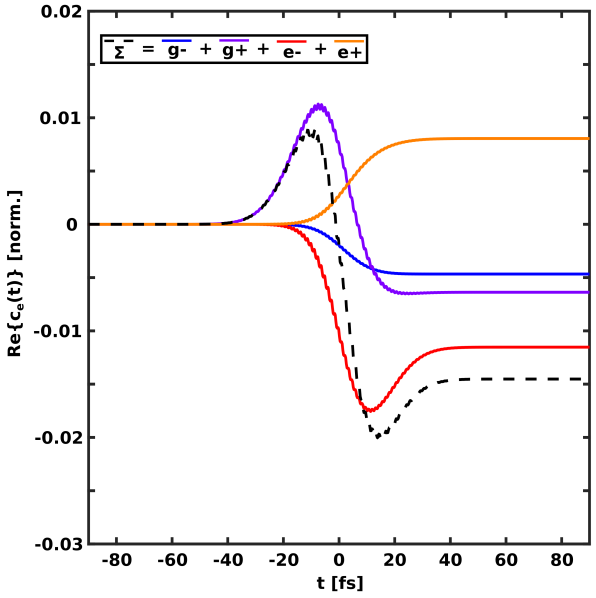

FIG. 4. Excited state coefficient contributions from the $\int VdU$ terms (RHS Eq. 13) normalized to the total final excited state coefficient. The imaginary complement is given by appendix Fig. 8.

[1] D. J. Tannor, *Introduction to Quantum Mechanics - A time-dependent perspective* (University Science Books, 2007).
[2] R. W. Boyd, *Nonlinear optics* (Academic press, 2019).
[3] T. Weinacht and B. Pearson, *Time-Resolved Spectroscopy: An Experimental Perspective*, Textbook series in physical sciences (CRC Press, Taylor & Francis Group, 2019), ISBN 9781498716734.

[4] M. Fewell, Optics communications **253**, 125 (2005).
[5] C. Trallero-Herrero, D. Cardoza, T. Weinacht, and J. Cohen, Physical Review A **71**, 013423 (2005).
[6] E. Brion, L. H. Pedersen, and K. Mølmer, J. Phys. A: Math. Theor. **40**, 1033 (2007), ISSN 1751-8113, 1751-8121.
[7] F. Reiter and A. S. Sørensen, Phys. Rev. A **85**, 032111 (2012), ISSN 1050-2947, 1094-1622.
[8] I. R. Sola, J. González-Vázquez, R. de Nalda, and L. Banares, Phys. Chem. Chem. Phys. **17**, 13183 (2015).
[9] W. D. M. Lunden, P. Sándor, T. C. Weinacht, and T. Rozgonyi, Phys. Rev. A **89**, 053403 (2014).
[10] M. Sala, in *Quantum Dynamics and Laser Control for Photochemistry* (Springer, 2016), pp. 107–127.
[11] B. W. Shore, Advances in Optics and Photonics **9**, 563 (2017).
[12] N. Mukherjee, W. E. Perreault, and R. N. Zare, in *Frontiers and Advances in Molecular Spectroscopy* (Elsevier, 2018), pp. 1–46.
[13] D. Finkelstein-Shapiro, D. Viennot, I. Saideh, T. Hansen, T. Pullerits, and A. Keller, Phys. Rev. A **101**, 042102 (2020), ISSN 2469-9926, 2469-9934.
[14] H. Friedmann and A. Wilson-Gordon, Optics Communications **24**, 5 (1978).
[15] D. Grischkowsky, M. Loy, and P. Liao, Physical Review A **12**, 2514 (1975).
[16] M. Krug, T. Bayer, M. Wollenhaupt, C. Sarpe-Tudoran, T. Baumert, S. S. Ivanov, and N. V. Vitanov, New Journal of Physics **11**, 105051 (2009).
[17] B. J. Sussman, American Journal of Physics **79**, 477 (2011).
[18] M. Göppert-Mayer, Annalen der Physik **401**, 273 (1931).
[19] M. Mrejen, H. Suchowski, T. Hatakeyama, C. Wu, L. Feng, K. O'Brien, Y. Wang, and X. Zhang, Nat Commun **6**, 7565 (2015), ISSN 2041-1723.
[20] B. T. Torosov and N. V. Vitanov, Phys. Rev. A **79**, 042108 (2009), ISSN 1050-2947, 1094-1622.
[21] V. Paulisch, H. Rui, H. K. Ng, and B.-G. Englert, Eur. Phys. J. Plus **129**, 12 (2014), ISSN 2190-5444.
[22] B. T. Torosov and N. V. Vitanov, J. Phys. B: At. Mol. Opt. Phys. **45**, 135502 (2012), ISSN 0953-4075, 1361-6455.
[23] P. Sándor, V. Tagliamonti, A. Zhao, T. Rozgonyi, M. Ruckenbauer, P. Marquetand, and T. Weinacht, Phys. Rev. Lett. **116**, 063002 (2016).

VII. APPENDIX

Appendix A: Adiabatic Elimination Full Derivation

Here we provide some details on the derivation of equations 11 based on the expression for the intemediate state given by equation 10. This includes the two-photon rotating wave approximation (TPRWA).

We start from the expression for the intermediate state, $c_i(t)$, that we arrived at in Eq. 10 from the main text:

$$\begin{aligned} c_i(t) =& \frac{-\chi_{gi}}{2} c_g(t) \left[\frac{e^{-i\omega_{g+}t}}{\omega_{g+}} + \frac{e^{-i\omega_{g-}t}}{\omega_{g-}} \right] \\ &+ \frac{-\chi_{ei}}{2} c_e(t) \left[\frac{e^{-i\omega_{e+}t}}{\omega_{e+}} + \frac{e^{-i\omega_{e-}t}}{\omega_{e-}} \right] \end{aligned} \tag{A1}$$

We insert Eq. A1 into the differential equations from Eq. 5 such that they can be reduced to two coupled differential equations given by:

$$i\dot{c_g} = A_{gg} c_g(t) + A_{ge} c_e(t) \tag{A2a}$$
$$i\dot{c_e} = A_{eg} c_g(t) + A_{ee} c_e(t) \tag{A2b}$$

where

$$\begin{aligned} A_{gg} &= \frac{\chi_{gi}\chi_{gi}}{4} \left(\frac{1 + e^{-i\omega_{g+}t} e^{+i\omega_{g-}t}}{\omega_{g+}} + \frac{e^{-i\omega_{g-}t} e^{+i\omega_{g+}t} + 1}{\omega_{g-}} \right) \\ A_{ge} &= \frac{\chi_{gi}\chi_{ei}}{4} \left(\frac{e^{-i\omega_{e+}t} e^{+i\omega_{g+}t} + e^{-i\omega_{e+}t} e^{+i\omega_{g-}t}}{\omega_{e+}} \right. \\ &\qquad \left. + \frac{e^{-i\omega_{e-}t} e^{+i\omega_{g+}t} + e^{-i\omega_{e-}t} e^{+i\omega_{g-}t}}{\omega_{e-}} \right) \\ A_{eg} &= \frac{\chi_{ei}\chi_{gi}}{4} \left(\frac{e^{-i\omega_{g+}t} e^{+i\omega_{e+}t} + e^{-i\omega_{g+}t} e^{+i\omega_{e-}t}}{\omega_{g+}} \right. \\ &\qquad \left. + \frac{e^{-i\omega_{g-}t} e^{+i\omega_{e+}t} + e^{-i\omega_{g-}t} e^{+i\omega_{e-}t}}{\omega_{g-}} \right) \\ A_{ee} &= \frac{\chi_{ei}\chi_{ei}}{4} \left(\frac{1 + e^{-i\omega_{e+}t} e^{+i\omega_{e-}t}}{\omega_{e+}} + \frac{e^{-i\omega_{e-}t} e^{+i\omega_{e+}t} + 1}{\omega_{e-}} \right) \end{aligned} \tag{A3}$$

The Hamiltonian for this AE two level system is:

$$H_{AE} = \begin{pmatrix} A_{gg} & A_{ge} \\ A_{eg} & A_{ee} \end{pmatrix} \tag{A4}$$

with the matrix elements given by Eqs. A3. We note that this Hamiltonian is not Hermitian. However, this is remedied by making the TPRWA.

We define the two-photon detuning as $\Delta_2 \equiv \omega_e - \omega_g - 2\omega_0 = \omega_{eg} - 2\omega_0$, then apply the TPRWA by neglecting all terms with frequencies oscillating faster than Δ_2. This requires us to evaluate each of the complex exponentials present in Eqs. A3. The possible resulting frequencies are shown in Table I as a matrix, where the first column and row show the AE frequencies and each subsequent cell is the AER frequency which is calculated by taking the difference of each row (m) with each column (n) or $m - n$. Where present the second line of a given cell is the first line rewritten in terms of Δ_2 to emphasize which combinations yield frequencies greater than Δ_2. The frequencies that remain after the approximation are shown in bold.

TABLE I. Rotating Wave Approximation

m ↓ | n →	ω_{g+}	ω_{g-}	ω_{e+}	ω_{e-}
ω_{g+}	**0**	$+2\omega_0$	$-\omega_{eg}$ $-(\Delta_2 + 2\omega_0)$	$\boldsymbol{-\omega_{eg} + 2\omega_0}$ $\boldsymbol{-\Delta_2}$
ω_{g-}	$-2\omega_0$	**0**	$-\omega_{eg} - 2\omega_0$ $-(\Delta_2 + 4\omega_0)$	$-\omega_{eg}$ $-(\Delta_2 + 2\omega_0)$
ω_{e+}	ω_{eg} $+(\Delta_2 + 2\omega_0)$	$\omega_{eg} + 2\omega_0$ $+(\Delta_2 + 4\omega_0)$	**0**	$+2\omega_0$
ω_{e-}	$\boldsymbol{\omega_{eg} - 2\omega_0}$ $\boldsymbol{+\Delta_2}$	ω_{eg} $+(\Delta_2 + 2\omega_0)$	$-2\omega_0$	**0**

Keeping only terms that oscillate at Δ_2 or slower, Eqs. A3 reduces to:

$$A_{gg} = \frac{\chi_{gi}^2}{2} \frac{\omega_{gi}}{\omega_{gi}^2 - \omega_0^2} = \omega_g^S(t) \tag{A5a}$$
$$A_{ge} = \frac{1}{4} \frac{\chi_{gi}\chi_{ei}}{\omega_{ei} - \omega_0} e^{-i\Delta_2 t} = \tilde{\Omega}(t) e^{-i\Delta_2 t} \tag{A5b}$$
$$A_{eg} = \frac{1}{4} \frac{\chi_{ei}\chi_{gi}}{\omega_{gi} + \omega_0} e^{+i\Delta_2 t} = \Omega(t) e^{+i\Delta_2 t} \tag{A5c}$$
$$A_{ee} = \frac{\chi_{ei}^2}{2} \frac{\omega_{ei}}{\omega_{ei}^2 - \omega_0^2} = \omega_e^S(t) \tag{A5d}$$

These matrix elements can be redefined as the dynamic Stark shift, $\omega_{g,e}^S(t)$, (Eqs. A5a and A5d) and the two-photon Rabi frequency, $\Omega(t)$, (Eqs. A5b and A5c). Thus we can write the Hamiltonian as

$$H_{AE+RWA} = \begin{pmatrix} \omega_g^S(t) & \tilde{\Omega}(t) e^{-i\Delta_2 t} \\ \Omega(t) e^{+i\Delta_2 t} & \omega_e^S(t) \end{pmatrix} \tag{A6}$$

with the matrix elements given by Eq. A5. This Hamiltonian is Hermitian in the limit that $\omega_{ei} - \omega_0 = \omega_{gi} + \omega_0$ or $\Delta_2 = 0$.

Inserting Eqs. A5 back into Eqs. A2 we generate the TDSE for AER given in the main text, Eq. 12.

Appendix B: Simulation Model

As discussed in the main text the simulation uses a differential equation solver to numerically integrate Eqs. 5 and 11 to calculate the state populations. The parameters used in Figs. 1 are given below in Table II.

We ran several simulations for varying pulse duration, $\Delta\tau_I$, as shown in Fig. 2, where we adjusted the pulse intensity, I_0, such that the pulse area was kept constant. All other parameters described in Table II remained the same.

TABLE II. Default Model parameters

Parameter	Value
E_g	0 THz
E_i	600 THz
E_e	800 THz
ν_0	400 THz
μ_{ig}	$2.11e^{-29}$ C · m
μ_{ie}	$2.09e^{-29}$ C · m
I_0	0.6667 TW/cm^2
$\Delta\tau_I$	30 fs

In a similar fashion, we varied the one-photon detuning, $\Delta = E_i - E_g - \nu_0$, by varying the intermediate state energy E_i. Fig. 5 shows the populations as a function of time with an inset displaying the energy level diagram. The four panels correspond to four different detunings: 50, 200, 350, and 500 THz, where the inset shows the intermediate state labelled $|i\rangle$ (purple) shifting to increasing energy. Once again the pulse intensity was adjusted to keep the pulse area constant and all other parameters described in Table II remained the same.

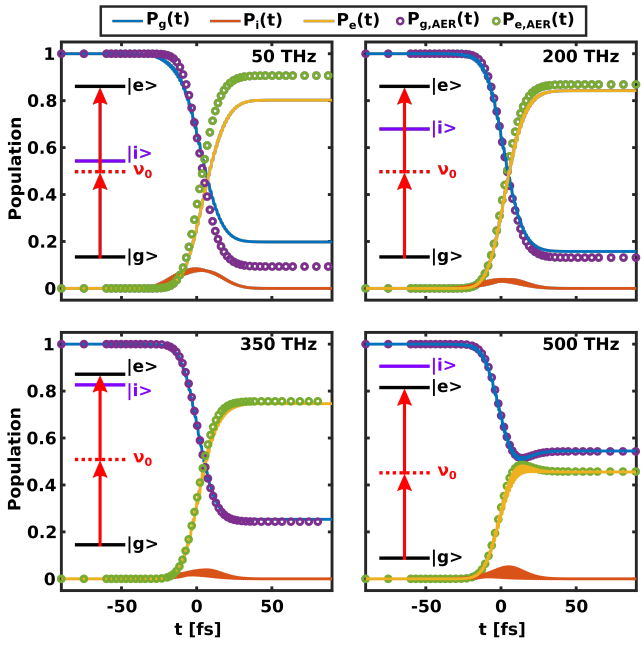

FIG. 5. Population as a function of time for four different detunings ($\Delta = |i\rangle - |\nu_0\rangle$) at 30fs pulse duration.

In terms of understanding adiabatic elimination, the pulse duration and one-photon detuning are interchangeable. To complement the qualitative nature of the comparison of the exact solution and AER described in Fig. 5, we calculated the population error as a function of detunings for a quantitative approach in Fig. 6. The figure shows an upper and lower x-axis which are coupled to one another. The lower axis describes the error in terms

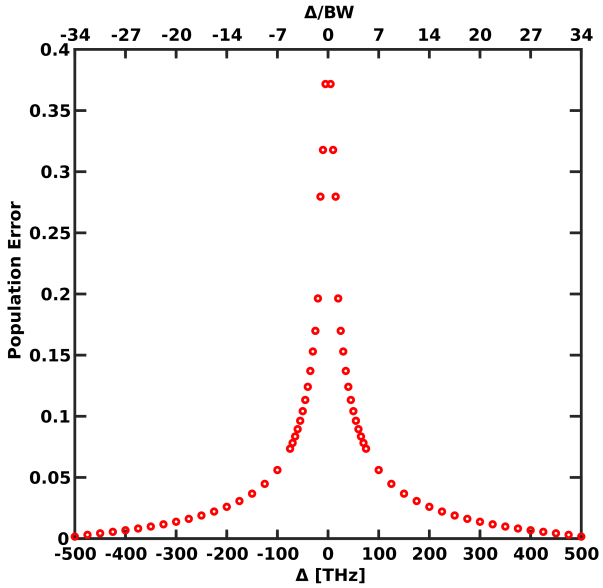

FIG. 6. Population error $((P_e - P_{e,AER})/P_e)$ as a function of one photon detuning with fixed pulse duration $FWHM = 30$ fs.

of the detuning, while the upper axis describes the error in terms of the SVEA. By dividing the detuning by the laser bandwidth for a 30 fs pulse we effectively re-write the SVEA as $\Delta/\chi >> 1$. From this graph one can see that even when the SVEA is no longer valid the error is still rather reasonable.

Appendix C: Imaginary Complement

Using the coefficients from the full solution we calculated each term that contributed to the total excited state coefficient. Figs. 3 and 4 show the real part normalized to $c_e(t)$. In Figs. 7 and 8 we show the complementary imaginary parts and note that the imaginary part is normalized to the final total excited state coefficient.

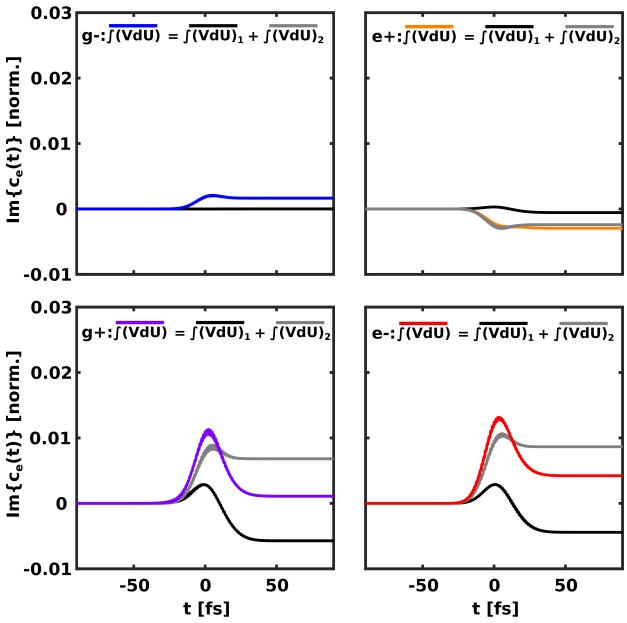

FIG. 7. Imaginary complement to figure 3.

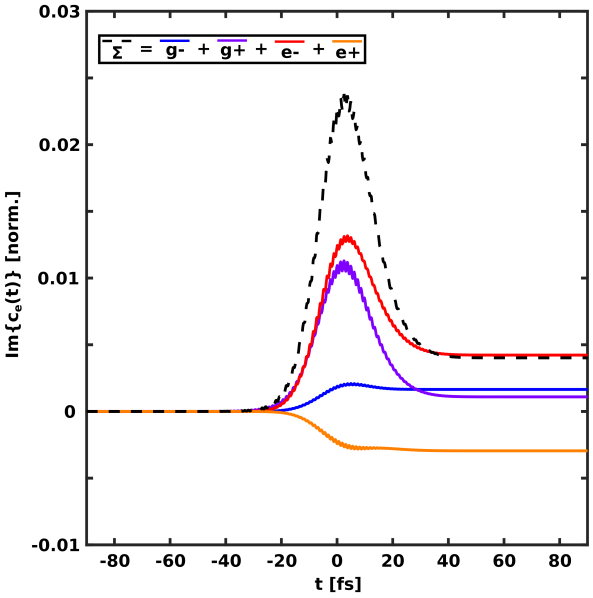

FIG. 8. Imaginary complement to figure 4.